Engineering Science and Technology, an International Journal 19 (2016) 1514–1525

HOSTED BY

Contents lists available at ScienceDirect

Engineering Science and Technology, an International Journal

journal homepage: www.elsevier.com/locate/jestch

Full Length Article

Modeling and analysis of hydraulic dashpot for impact free operation in a shut-off rod drive mechanism

Narendra K. Singh [a,*], Deepak N. Badodkar [a,b]

[a] Division of Remote Handling and Robotics, Bhabha Atomic Research Centre, Mumbai 400085, India
[b] Homi Bhabha National Institute, Anushaktinagar, Mumbai 400094, India

ARTICLE INFO

Article history:
Received 29 December 2015
Revised 11 May 2016
Accepted 11 May 2016
Available online 21 May 2016

Keywords:
Hydraulic dashpot
Rigid body dynamics
Nuclear reactor
Reactor control mechanism
Rod drop profile
Shut-off rods

ABSTRACT

Rotary hydraulic dashpot used for shut-off rod drive mechanism application of a nuclear reactor has been studied in this paper for impact free operation. The rotary hydraulic dashpot has been modeled as a system with 1 degree of freedom (DOF) and the simulation results are experimentally validated. The dashpot is modeled as a hinge joint with moving and fixed vanes as rigid bodies. Shut-off rods are used to shut-down a nuclear reactor and hydraulic dashpot absorbs the energy of freely falling shut-off rod at the end of rod travel. With the increase in the environmental temperature the dashpot becomes underdamped at a point because of reduction in the viscosity of oil and results into impact on mechanism components. Hydraulic dashpot designs are finalized with an optimum combination of dashpot clearances and oil viscosity to meet the drop time criterion and impact free operation at room temperature as well as at elevated temperature. Also with the change in mechanical loads the dashpot becomes underdamped. So the study is further extended to see the effects of various parameters such as moment of inertia, constraint angle and applied moment on the dashpot. Study is focused on obtaining dashpot responses in terms of relative rotation, relative angular velocity and relative angular acceleration at various environmental temperatures. Finite element commercial code COMSOL Multiphysics 5.1 has been used for numerical simulations. Equations for both rigid body dynamics and heat transfer in solids are solved simultaneously. Thus, energy absorbed and local temperature rise in the dashpot operation is also obtained. Both simulation and experimental results at wide range of environmental temperature are presented and compared in this paper. This study forms a good tool to design a hydraulic dashpot, which gives impact free operation in a shut-off rod free fall.

1. Introduction

Nuclear reactors are shut-down by inserting shut-off rods inside the reactor core and these rods are moved using shut-off rod drive mechanisms (SRDM). At the time of reactor start-up, rods are withdrawn at a given speed and are held in position during the reactor operation. On demand, shut-off rods fall freely into the reactor core. However, at the end of rod travel, rod velocity is smoothly brought to zero using a passive device called as 'Hydraulic Dashpot'. In this, damping oil is allowed to flow from one chamber to the other through narrow clearances, giving damping action. After dashpot engagement, there is a sudden pressure built-up inside the high pressure chamber and thereafter it reduces at the end of travel as oil passes to low pressure chamber through narrow clearances. The hydraulic dashpot vanes rotate typically by 120° in one rod drop cycle. General arrangement of SRDM along with the guide tube components is given in Fig. 1. The detailed study of dashpot pressure and damping force in the hydraulic dashpot is presented in Singh et al. [1]. These mechanisms are to be qualified at room temperature during reactor start-up as well as at elevated temperature during reactor operation, where heat comes from environment. Hydraulic dashpot designs are finalized with an optimum combination of dashpot clearances and oil viscosity. These hydraulic dashpots are a part of safety critical system, hence required to operate in a passive manner. Active shock absorbers like based on magneto-rheological (MR) fluids as given by Kumbhar et al. [2] are not suitable for shut-off rod drive mechanism applications.

Wenzer [3] has done the analysis of dashpot performance for rotating control drums of a lithium cooled fast reactor concept, where with manual calculation the available torque was calculated at every time step and dashpot rotational velocity vs time curves

* Corresponding author.
E-mail addresses: nksingh_chikki@yahoo.com, narens@barc.gov.in (N.K. Singh).
Peer review under responsibility of Karabuk University.

http://dx.doi.org/10.1016/j.jestch.2016.05.005
2215-0986/

Nomenclature

A	total vane area
cc	cubic centimeter
C_p	specific heat capacity at constant pressure
°C	degree Celsius
c_θ	damping coefficient
cst	centistokes
Fig.	figure
I	unit matrix
J	Joule
I_e	effective moment of inertia at the joint
I_{src}	source moment of inertia
I_{dest}	destination moment of inertia
ID	inner diameter
k	coefficient of thermal conductivity
°K	degree Kelvin
kg	kilogram
k_θ	spring constant
m	meter
mm	millimeter
M	total dashpot moment
M_d	damping moment
N	Newton
No.	number
OD	outer diameter
p	pressure
p_u	penalty factor
Pa	Pascal
Q	heat sources
R	rotation matrix
R_t	torque arm
rad	radian
$\mathbf{R}_{\text{src}}$	rotation matrices describing the rotation of source attachments
$\mathbf{R}_{\text{dest}}$	rotation matrices describing the rotation of destination attachments
s	second
t	time
T	absolute temperature
T_q	torque
u	displacement field
$\mathbf{u}_{\text{con}}$	convective velocity field
$\mathbf{u}_{\text{c.src}}$	displacement vectors for source attachments
$\mathbf{u}_{\text{c.dest}}$	displacement vectors for destination attachments
$\mathbf{u}_{\text{src}}$	displacements at the centroid of the source attachments
$\mathbf{u}_{\text{dest}}$	displacements at the centroid of the destination attachments
V	volt
$\mathbf{X}_{\text{c}}$	joint center
$\mathbf{X}_{\text{c.src}}$	positions of centroids for source attachments
$\mathbf{X}_{\text{c.dest}}$	positions of centroids for destination attachments
w.r.t.	with respect to
W	Watt
W_d	energy dissipation rate

Greek symbols

ρ	density of fluid
∇	divergence
Φ_{src}	rotation about the axis for source attachments
Φ_{dest}	rotation about the axis for destination attachments
ω	angular velocity
θ	relative rotation
θ_0	pre-deformation

Abbreviation

AHWR	advanced heavy water reactor
CFD	computational fluid dynamics
DOF	degree of freedom
EM	electro-magnetic
MWe	megawatt electric
PHWR	pressurized heavy water reactor
RPM	rotation per minute
SRDM	shut-off rod drive mechanism

were generated. With advancement in computational techniques, various researchers have developed damper models and simulations were done. Suresh et al. [4] has done the performance analysis of oil dashpot in control and safety rod drive mechanism. Analysis is done by mathematical modeling of dashpot system as spring mass damper two degree of freedom system. A basic model of a control assembly drop in nuclear reactors is given by Bulin et al. [5]. They have proposed two models; one is a simple rigid body model intended for basic dynamic analysis and other is based on complex multibody model. Allen et al. [6] have developed a damper model for use in multi-body model for use in multi-body dynamic simulations. In this study a warrior armoured personnel carrier rotary damper is modeled. They also studied the responses of damper at different flow regimes. Lion and Loose [7] have given a thermo-mechanically coupled model for automotive shock absorber. Jingyang et al. [8] have done multi-body dynamic simulation of flapping wing. In this study, the inertial force and inertial moment between the wing and the body are reflected in the simulation model and the multi-body dynamic equation of model is presented. Shabana [9] has done the viscoelastic analysis of multi-body systems using FEM. In his study constraints between components are formulated.

Present study includes modeling of hydraulic dashpot as a system with 1 DOF, simulation, experimental studies and parametric studies. Dashpot response curves in terms of relative rotation; relative angular velocity; and relative angular acceleration are obtained. The study is done to see the performance of the hydraulic dashpot up to 85 °C. The impact in the hydraulic dashpot beyond 55 °C is also studied. Energy absorbed in dashpot and temperature rise is also studied. Simulation and experimental results are compared. Parametric study is also done using dashpot model. The method used to model the hydraulic dashpot and results obtained are novel. This study forms a handy tool to analyze the performance of rotary hydraulic dashpot.

2. Study set-up description

The present study is carried-out on a prototype SRDM and full-scale test set-up meant to qualify the shut-off rod drive mechanism of 'Critical Facility' reactor. Shut-off drive mechanism design is to be qualified on a full scale test station as a regulatory guideline, discussed in Singh [10]. In the shut-off rod drive mechanism, internally the motor sub-assembly is connected to a worm gear and an electromagnetic (EM) clutch sub assembly, which is further connected to a sheave through a set of spur gears. Absorber element (shut-off rod) is mounted on the sheave through a wire rope. EM clutch is energized to raise the rod through motor. As soon as the rod reaches the top position, motor is cut-off and the rod remains at that position, due to irreversibility of worm gear design. During reactor scram, the EM clutch is de-energized and rod falls freely

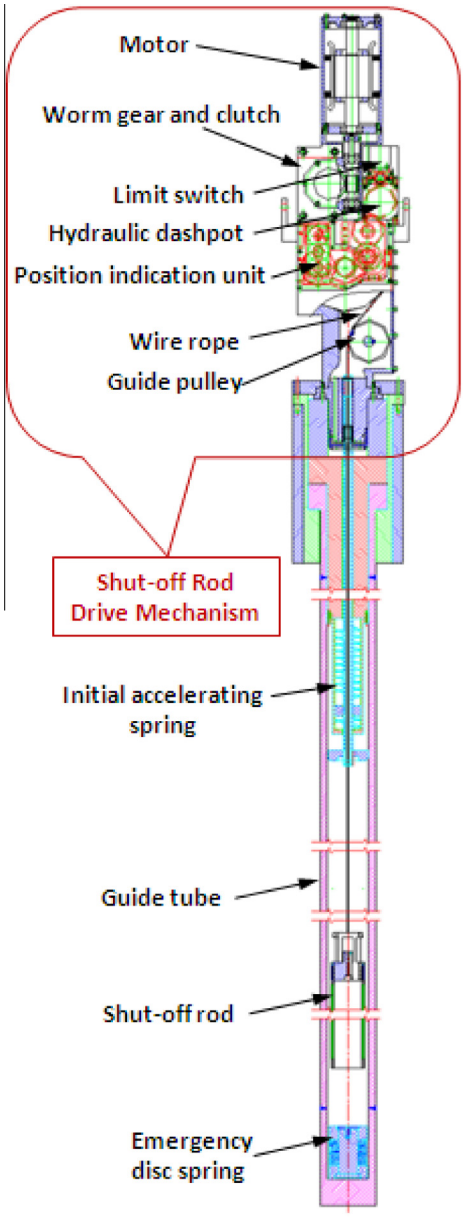

Fig. 1. General arrangement of shut-off rod drive mechanism along with the guide tube components.

due to gravity. Taliyan et al. [11] have studied the dynamics of rod drop in detail. A set of pick-up rings are used, which lapse one over the other bringing hydraulic dashpot into action precisely at the desired position (typically 90% of rod drop). A spiral spring is used for resetting the hydraulic dashpot during rod withdrawal. Fig. 2 gives the detailed construction of hydraulic dashpot studied. All the parameters of the hydraulic dashpot under study are given in Table 1.

For dashpot performance analysis, we need equivalent moment of inertia at the dashpot shaft, damping coefficient and spring constant of the hydraulic dashpot. For calculating the equivalent moment of inertia at the dashpot shaft, the moment of inertia of each and every rotating component is resolved into the moment of inertia at the dashpot shaft as given in Taliyan et al. [11].

Damping coefficients of dashpot at various temperatures have been calculated from the experimental and CFD results. Values of pressure and relative angular rotation are taken from the experimental results. The values of damping coefficients are calculated as below:

$$c_\theta = T_q/\omega \tag{1a}$$

$$c_\theta = p \cdot A \cdot R_t/\omega \tag{1b}$$

where c_θ is the damping coefficient (N m s/rad), T_q is torque (N m), ω is the angular velocity (rad/s), p is the pressure (N/m^2), A is the total vane area (m^2) and R_t is the torque arm (m). Torque arm is the distance between center of shaft and the center of vane face.

For a particular experimental result, damping coefficients are calculated at different time steps. The values of damping coefficients at different time steps of dashpot operation are plotted and mean value of the damping coefficient is taken into consideration. Fig. 3 gives the variation of damping coefficient vs time at 35 °C. The value of spring constant (N m/rad) is measured experimentally with the help of a torque wrench. Values of equivalent moment of inertia, spring constant and damping coefficients at different environmental temperatures are also given in Table 1.

3. Multibody dynamics modeling and simulations

3.1. Modeling procedure

Finite element commercial code COMSOL Multiphysics 5.1 is used to model the hydraulic dashpot. COMSOL 5.1 documentation [12] and tutorials [13,14]. Fixed vanes in the hydraulic dashpot are attached to the housing and the moving vanes are attached to the rotating shaft and there is no axial movement along the axis of the shaft. These vanes are modeled as two arms of hinge joint. The hinge joint, also known as a revolute joint has one rotational degree of freedom between the two components. The two components are free to rotate relative to each other about the axis of the joint. The stresses in the dashpot components are not of interest in present study, so the dashpot moving vanes along with shaft and dashpot fixed vanes along with housing are modeled as rigid domain. Spring and damper are applied between the arms of the hinge joint. Rotation of the arm is also constrained to 120° as there is a mechanical stopper in the dashpot at 120°. To see the effects of all relative motion (including vane side relative motion) in the hydraulic dashpot, the modeling is done in 3-D. Energy variation in the dashpot operation is studied. Local increase in temperature during operation is also studied. Time dependent study is performed. Fig. 4 shows the dynamic model of hydraulic dashpot. Based on requirements, analysis strategy has been formulated in which following two physics aspects of COMSOL have been solved simultaneously:

- Multibody dynamics (Rigid body dynamics).
- Heat transfer in solids.

3.2. Theory and governing equations

An attachment is a set of boundaries on a flexible component used to connect it to another flexible component or a rigid component through a joint. The attachment center of rotation is the centroid of its selected boundaries. In a joint, it is possible to select the attachment center of rotation as the center of the joint. The forces and moments on an attachment are computed by summing the reaction forces on the selected boundaries. These forces and moments are used to evaluate the joint forces.

A four parameter *quaternion* representation is used for rotations in COMSOL. The connection between the quaternion parameters and rotation matrix ($\mathbf{R}$) is established. Under pure rotation, a vector from the center of rotation ($\mathbf{X}_c$) of the attachment to a point $\mathbf{X}$ on the undeformed solid will be rotated into:

$$\mathbf{x} - \mathbf{X}_c = \mathbf{R}(\mathbf{X} - \mathbf{X}_c) \tag{2a}$$

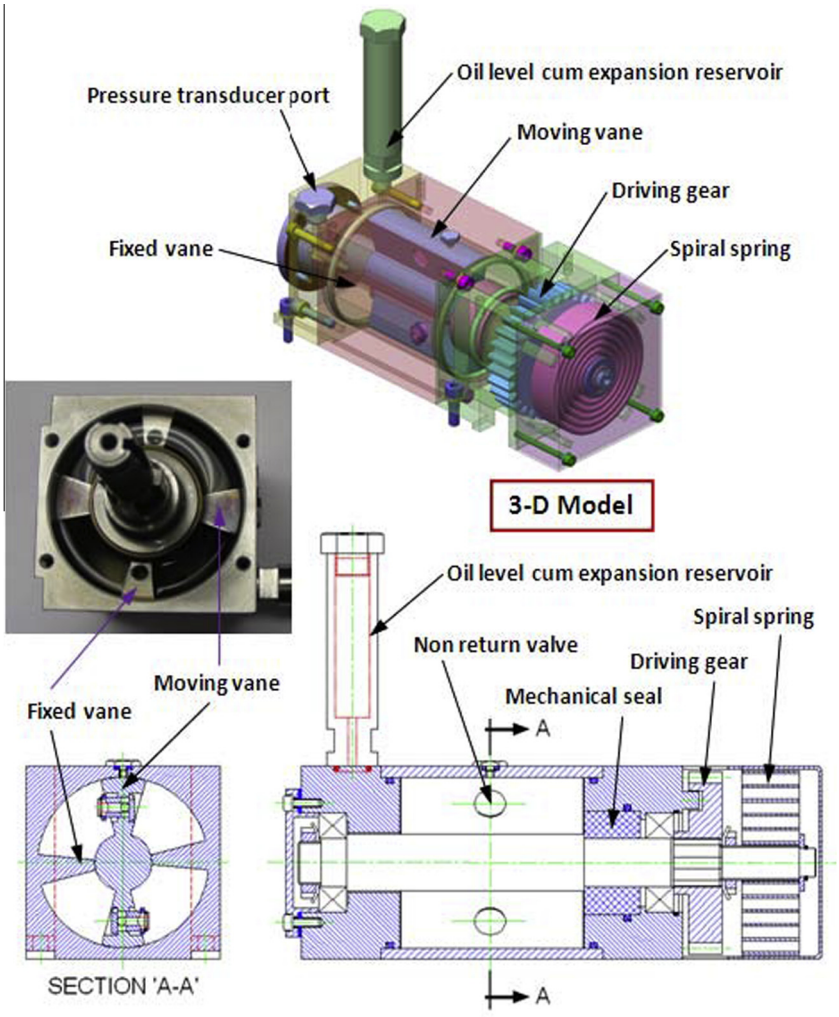

Fig. 2. Detailed construction of hydraulic dashpot.

Table 1
Study set-up parameters.

Parameter	Value for 'Critical Facility' reactor
Drive mechanism overall size (mm)	210 × 196 × 750
Hydraulic dashpot vane size (mm)	20 ID × 60 OD × 64.6 Long
Rod travel (mm)	2400
Rod weight (kg)	8
Free fall (mm)	2160 (in air)
Approximate volume of the oil (cc)	162
Hydraulic dashpot rotation (degree)	120
Mechanical shaft seal	On one side
No. of dashpot vanes	Two moving vanes/two fixed vanes
Shaft and moving vane material	SS 17.4 PH
Housing and fixed vane material	SS 17.4 PH
Viscosity of oil used at 25 °C (cst)	1500
Mass of moving vane (kg)	0.53
Equivalent moment of inertia ($kg\ m^2$)	0.1929
Spring constant (N m/rad)	0.93
Environment temperature (°C)	35 45 55 65 75 85
Damping coefficient (N m s/rad)	4.51 4.11 3.30 3.22 3.16 3.11

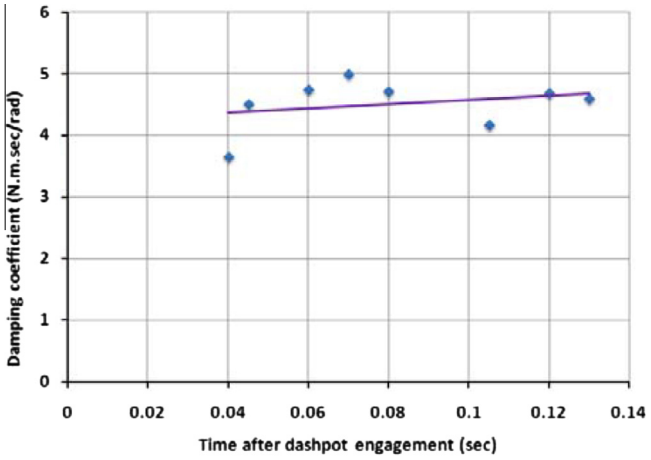

Fig. 3. Variation of damping coefficient vs time at 35 °C.

where **x** is the new position of the point, originally at **X**.

The displacement is by definition

$$\mathbf{u} = \mathbf{x} - \mathbf{X} = (\mathbf{R} - \mathbf{I})(\mathbf{X} - \mathbf{X}_c) \quad (2b)$$

where **I** is the unit matrix. Scheme of position vectors under pure rotation is shown in Fig. 5(a). All position vectors are defined w.r.t. origin.

When the center of rotation of the attachment also has a translation $\mathbf{u}_c$, then the complete expression for the displacements on the solid is

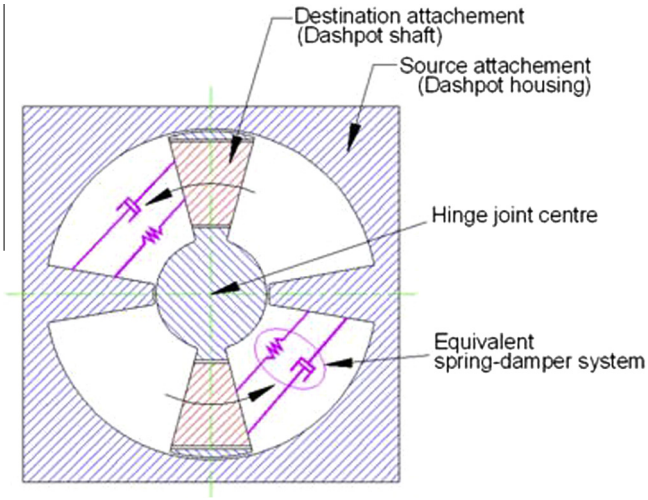

Fig. 4. Dynamic model of hydraulic dashpot.

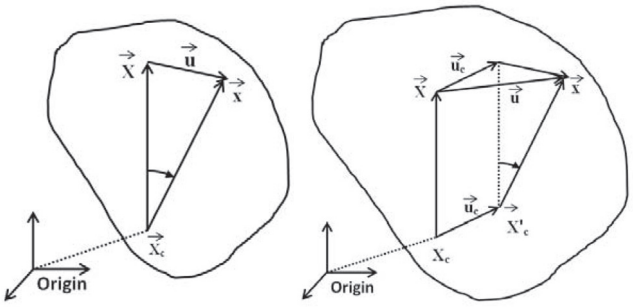

(a) Under pure rotation (b) Under combined rotation and translation

Fig. 5. Scheme of position vectors.

$$\mathbf{u} = \mathbf{u}_c + (\mathbf{R} - \mathbf{I})(\mathbf{X} - \mathbf{X}_c) \tag{2c}$$

Scheme of position vectors under combined rotation and translation is shown in Fig. 5(b). $\mathbf{X}'_c$ is the new position of center of rotation of the attachment after translation.

For a hinge joint, the destination attachment is free to rotate relative to the source attachment about the joint axis. The relative rotation about the joint axis (θ) is the degree of freedom. To formulate this kind of connection, the motion of destination attachment is prescribed in terms of the motion of the source attachment as follows:

$$\mathbf{u}_{c.dest} = \mathbf{u}_{c.src} \tag{2d}$$

$$\Phi_{dest} = \Phi_{src} + \theta \tag{2e}$$

$$\mathbf{u}_{c.src} = \mathbf{u}_{src} + (\mathbf{R}_{src} - \mathbf{I})(\mathbf{X}_c - \mathbf{X}_{c.src}) \tag{2f}$$

$$\mathbf{u}_{c.dest} = \mathbf{u}_{dest} + (\mathbf{R}_{dest} - \mathbf{I})(\mathbf{X}_c - \mathbf{X}_{c.dest}) \tag{2g}$$

where $\mathbf{u}_{c.src}$ and $\mathbf{u}_{c.dest}$ are the displacement vectors for source and destination attachments and $\mathbf{u}_{src}$ and $\mathbf{u}_{dest}$ are the displacements at the centroid of the source and destination attachments. $\mathbf{X}_c$ is the joint center, $\mathbf{X}_{c.src}$ and $\mathbf{X}_{c.dest}$ are the positions of centroids for source and destination attachments. $\mathbf{R}_{src}$ and $\mathbf{R}_{dest}$ are the rotation matrices describing the rotation of source and destination attachments, Φ_{src} and Φ_{dest} are the rotation about the axis for source and destination attachments. $\mathbf{I}$ is the unit matrix.

Forces and moments at center of joint due to input parameters will be balanced by the dashpot moment. Total dashpot moment (due to spring and damper) can be given as:

$$M = -k_\theta(\theta - \theta_0) - c_\theta\left(\frac{\partial\theta}{\partial t}\right) \tag{3}$$

where M is the total dashpot moment (N m), k_θ is the spring constant (N m/rad), c_θ is the damping coefficient (N m s/rad), θ is relative rotation (rad), θ_0 is the pre-deformation (rad) and t is time (s).

The Eqs. (2d)–(2g) are general equations for hinge joint, while Eq. (3) is equation for spring damper system.

The constraint on the relative displacement is enforced using a stiff spring between the components. The stiffness of the spring is defined by the penalty factor. The penalty factor (p_u) is evaluated as below:

$$p_u = \left[\frac{\frac{d\theta}{dt}}{\delta\theta\_max}\right]^2 I_e \tag{4a}$$

where θ is relative rotation, t is time. The numerator in the Eq. (4a) is an assumed angular velocity between the components when the constraint is applied, and the denominator is the maximum allowable penetration. This ratio of the relative angular velocity and the maximum allowable penetration decides the required stiffness of the spring (the penalty factor). The factor I_e in the Eq. (4a) is the effective moment of inertia at the joint, defined as:

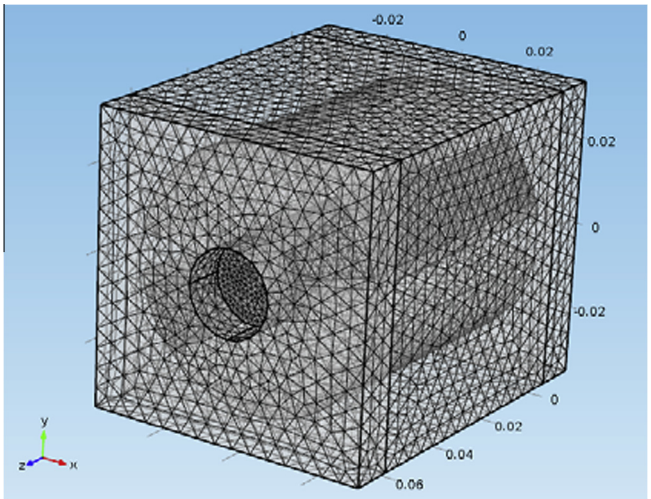

Fig. 6. A typical mesh of hydraulic dashpot assembly.

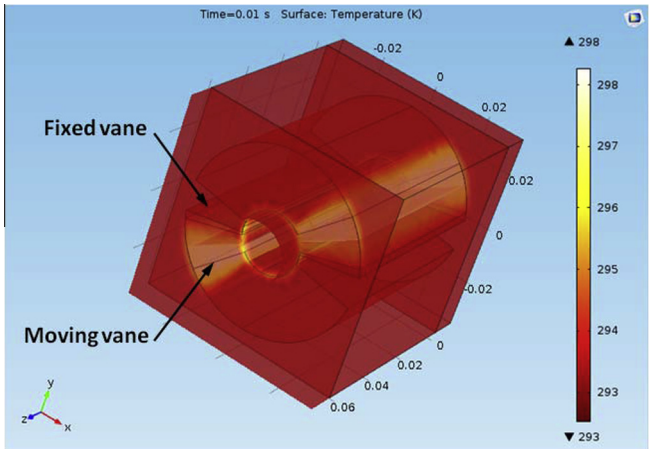

Fig. 7. 3-D Temperature profile of hydraulic dashpot.

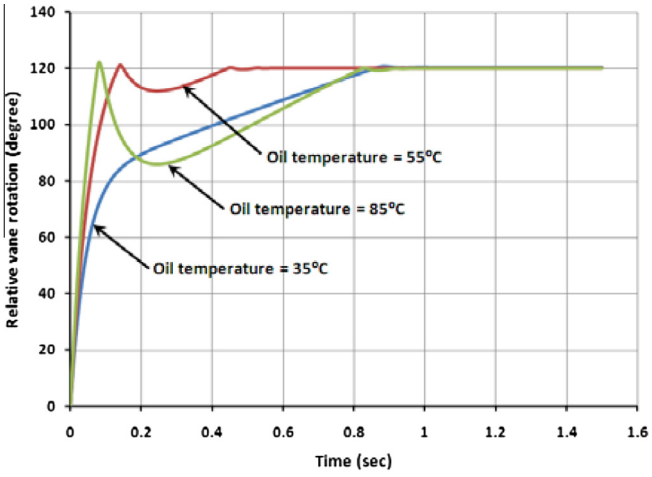

Fig. 8. Relative vane rotation vs time.

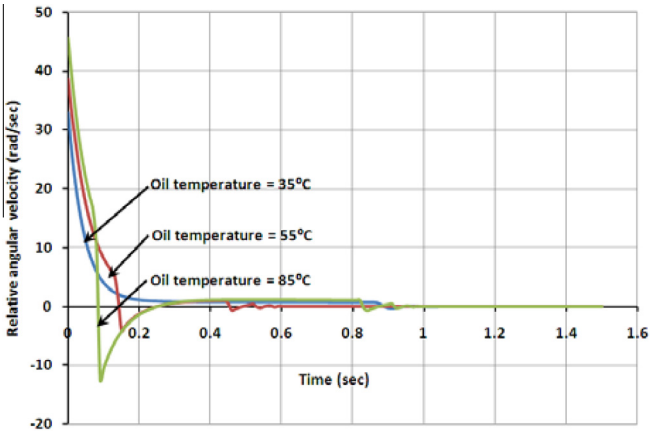

Fig. 9. Relative angular velocity vs time.

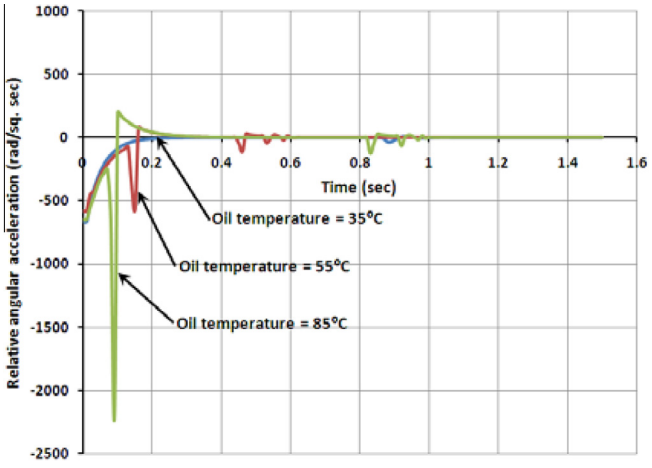

Fig. 10. Relative angular acceleration vs time at 35 °C.

$$I_e = \frac{(I_{src} I_{dest})}{(I_{src} + I_{dest})} \tag{4b}$$

where I_{src} and I_{dest} are source and destination moment of inertias.

From Eq. (3) damping moment (M_d), as given in [12] and Thomson and Dahleh [15], is $c_\theta \left(\frac{\partial \theta}{\partial t}\right)$

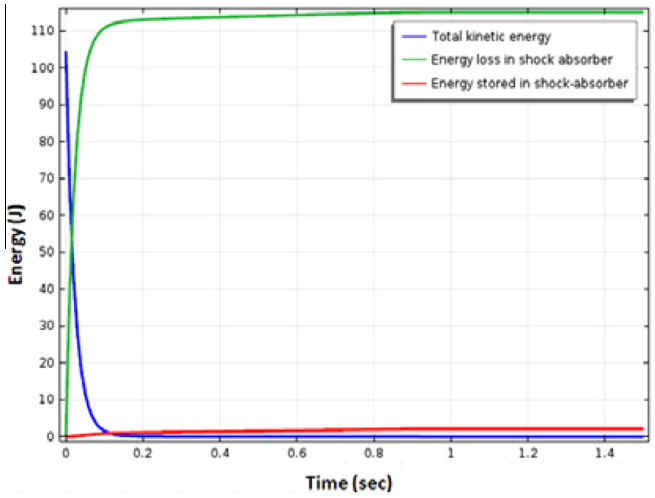

Fig. 11. Variation of energy vs time at 35 °C.

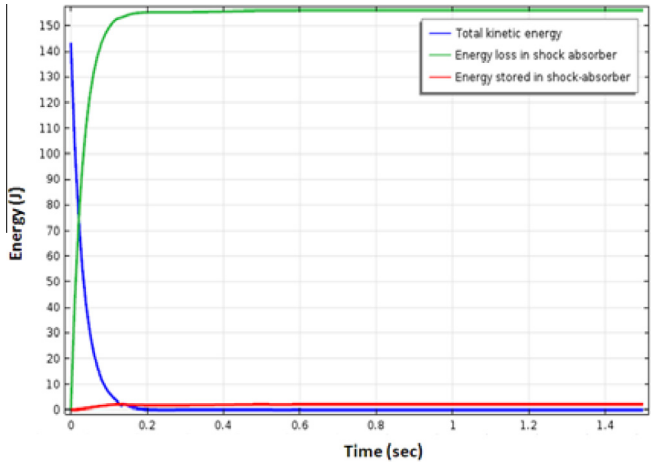

Fig. 12. Variation of energy vs time at 55 °C.

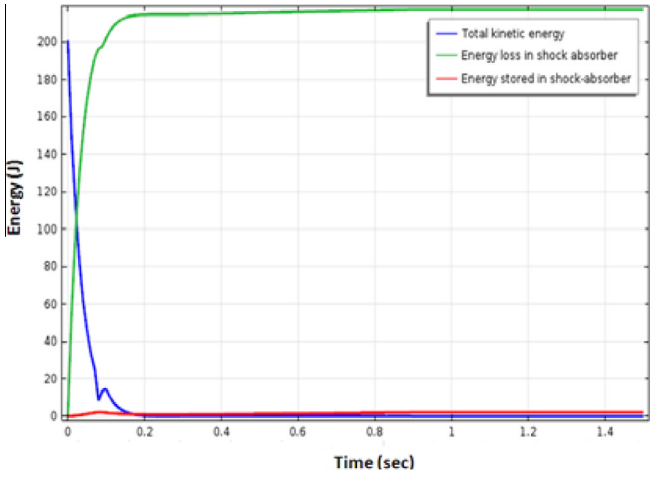

Fig. 13. Variation of energy vs time at 85 °C.

Further, energy dissipation rate (W_d) can be given as $c_\theta \left(\frac{\partial \theta}{\partial t}\right)^2$

Total energy lost in the dashpot will be converted into heat and give temperature rise. This energy dissipation rate which comes from rigid body dynamics will act as a heat source in the energy

Table 2
Simulation results.

Temperature (°C)	Time taken for 120° rotation (s)	Initial kinetic energy (J)	Total Energy loss in shock absorber (J)	Impact in the dashpot	Vane hitting velocity (rad/s)
35	0.86	104	115	No	–
45	0.52	123	134	No	–
55	0.15	144	156	Yes	5.4
65	0.10	176	190	Yes	8.9
75	0.08	196	212	Yes	13.2
85	0.07	201	216	Yes	15.1

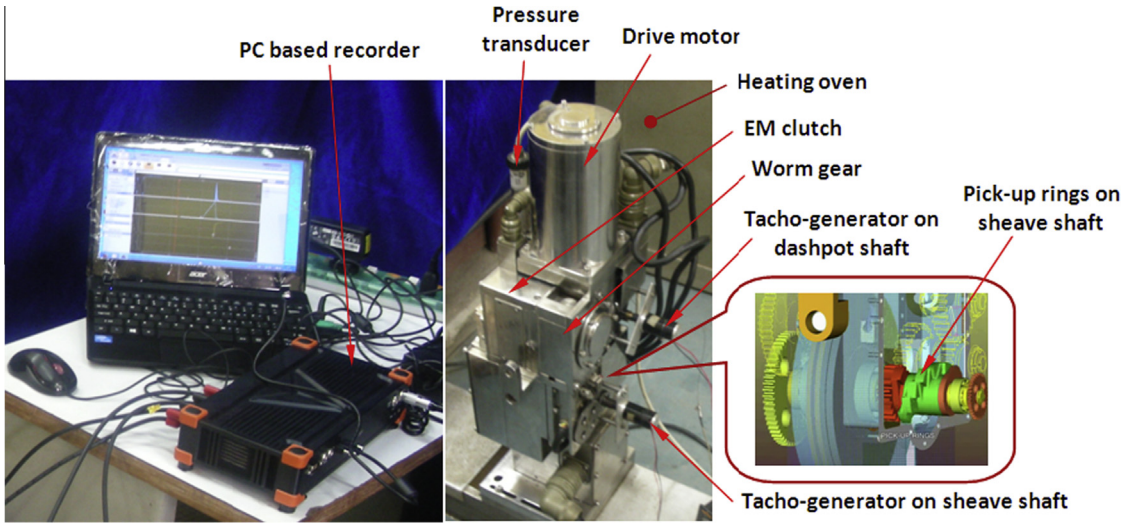

Fig. 14. Test set-up for experimental studies.

equation. To get the temperature rise during the dashpot operation, energy equation is solved in the heat transfer in solids interface of COMSOL. Time dependent general energy equation as given in [12] and Bird et al. [16] is:

$$\rho C_p \frac{\partial T}{\partial t} + \rho C_p \mathbf{u}_{\text{con}} \cdot \nabla T = \nabla \cdot (k \nabla \text{T}) + Q \tag{5}$$

where ∇ is divergence, ρ is density of dashpot fluid (kg/m^3), C_p is specific heat capacity at constant pressure (J/kg K), k is coefficient of thermal conductivity (W/m K), T is the absolute temperature (°K), $\mathbf{u}_{\text{con}}$ is the convective velocity vector (m/s) and Q is heat sources (W/m^3).

However, for heat transfer in solids, convective term becomes zero, hence the time dependent energy equation for solids as used by Asif et al. [17] reduced to:

$$\rho C_p \frac{\partial T}{\partial t} = \nabla \cdot (k \nabla T) + Q \tag{5′}$$

Total heat loss in the shock absorber will be the time integration of heat generated per second and will give rise to the local temperature. Energy stored in shock absorber will be multiplication of spring constant and its rotation. All these parameters are defined in the variables.

3.3. Boundary conditions

Dashpot housing along with fixed vanes (rigid domain 2) is given as fixed constraint boundary condition. Moving vanes along with shaft (rigid domain 1) is given as following boundary conditions:

- Initial values: Initial angular velocity acquired by the moving vane.
- Applied moment: Moment equivalent to weight of the absorber element constantly acting on the dashpot shaft.
- Mass and moment of inertia: Mass of the dashpot shaft and the equivalent moment of inertia of all rotating parts derived on the dashpot shaft.

Hinge joint is applied between the two rigid domains. Rigid domain 2 (fixed vane) is given as source attachment while rigid domain 1 (moving vane) is given as destination attachment. Spring and damper system is applied between the two rigid domains. Rotational constraint boundary condition for 120° is applied in the hinge joint to restrict the rotation beyond 120°.

Moving and fixed domains in the model are assembled with identity pair. All the surfaces which are in relative motion are defined as identity pair. For heat transfer in solids, pair boundary heat source boundary condition is applied on the identity pair, as this is the source of heat generation.

3.4. Mesh sensitivity and convergence methods

A mesh sensitivity study is performed to find the mesh size that was sufficiently fine so that solution does not change by further refining the mesh. Tetrahedral mesh with varying mesh density as shown in Fig. 6 is chosen for study. Response curves, local temperature and energy variation was evaluated at different mesh sizes. Response curves (motion) are not influenced by mesh density as all domains are considered as rigid body for dynamics aspects, but it will influence the temperature rise as domains for heat transfer solids are not modeled as rigid body. No appreciable

Table 3
Experimental results.

Environment temperature (°C)	Sheave shaft peak angular velocity (rad/s)	Dashpot peak angular velocity (rad/s)	Dashpot peak pressure (bar)	Peak damping moment due to pressure (N m)	Damping coefficient (N m s/rad)	Impact in the dashpot action	Vane hitting velocity (rad/s)	Drop time for 90% travel (s)	Drop time for 100% travel (s)
35	71.01	32.67	12.97	67.02	4.51	No	–	1.02	2.22
45	70.74	35.50	11.85	61.24	4.11	No	–	1.00	1.70
55	70.86	38.30	10.85	56.07	3.30	Yes	7.74	0.99	1.15
65	71.45	42.48	9.57	49.45	3.22	Yes	9.02	0.98	1.12
75	71.31	44.72	9.00	46.51	3.16	Yes	10.47	0.98	1.10
85	72.12	45.31	8.90	45.99	3.11	Yes	12.56	0.97	1.08

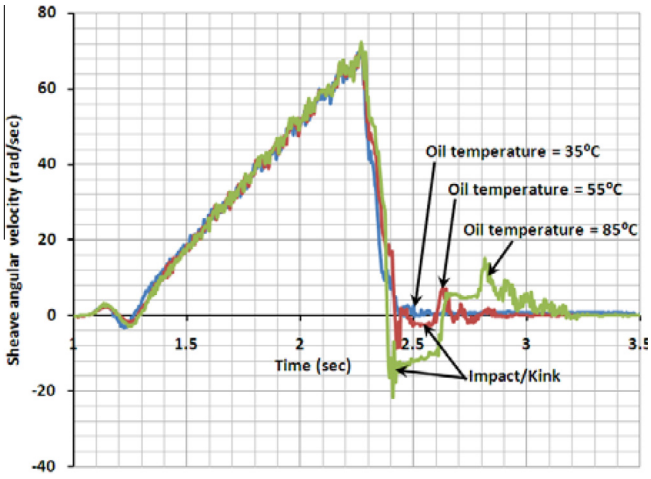

Fig. 15. Experimental sheave angular velocity vs time.

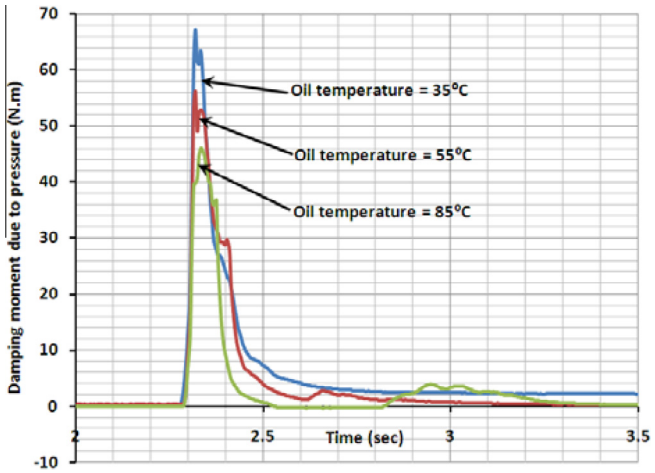

Fig. 17. Experimental variation of damping moment due to pressure vs time.

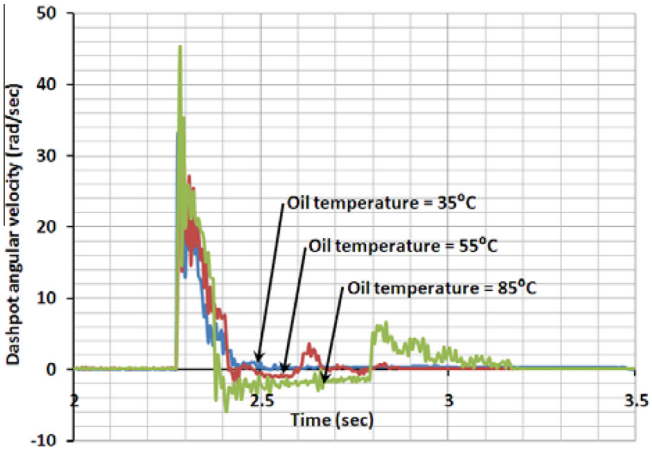

Fig. 16. Experimental dashpot response (angular velocity) vs time.

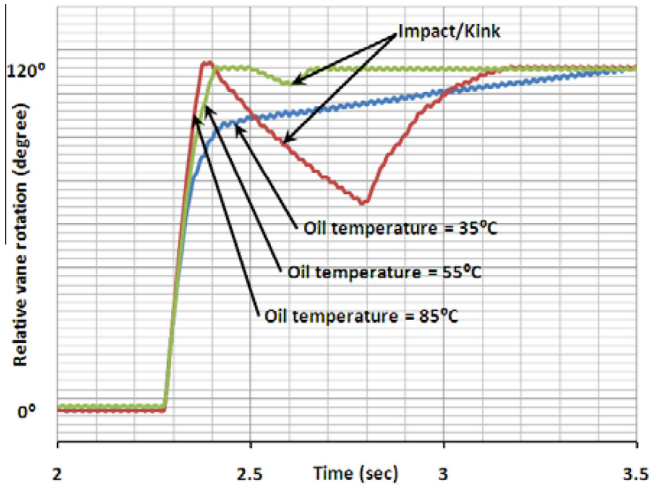

Fig. 18. Experimental dashpot relative vane rotation vs time.

change has been found beyond 108,095 numbers of elements. So this is considered as the optimized mesh size for this study. Both rigid body dynamics and heat transfer in solids interfaces are solved simultaneously. Time dependent iterative (geometric multi-grid) solvers are used with segregated approach. Temperature is kept in segregated step 1 while other variables are kept in segregated step 2. Nonlinear methods used for both segregated approaches are Constant (Newton). All the solutions were considered to be fully converged when the sum of residuals was below 10^{-5}. Convergence was achieved on a work station with system descriptions as: Processor; 3.40 GHz, 64-bit operating system and 64.0 GB RAM.

3.5. Simulation results

Simulation results are shown in Figs. 7–13. Fig. 7 shows the 3-D temperature profile of the hydraulic dashpot. Fig. 8 gives relative vane rotation vs. time, Fig. 9 gives relative angular velocity vs time and Fig. 10 gives relative angular acceleration vs time. At 35 °C, the relative rotation of the vane is fast initially, and then it rotates slowly towards the end of the travel as by this time the energy is absorbed by the dashpot and vane rotates because of absorber element weight only. It is clear from the relative angular velocity curves that, at 35 °C, the vane rotation is smooth at the end of

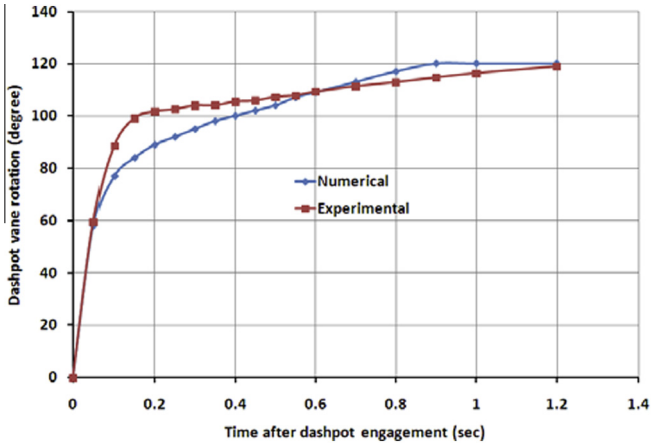

Fig. 19. Comparison of numerical and experimental dashpot vane rotation vs time at 35 °C.

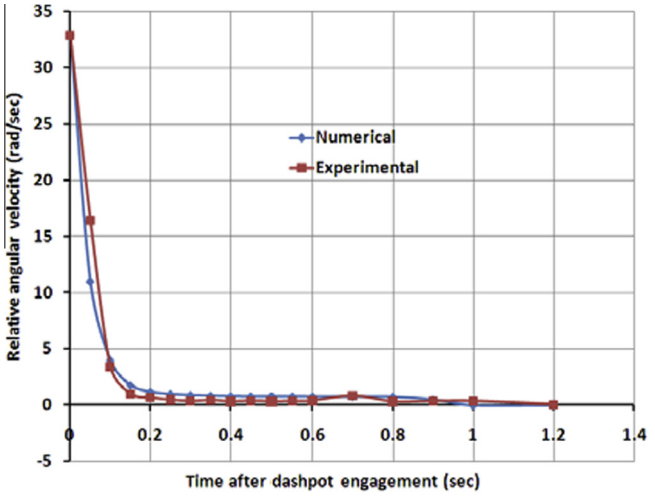

Fig. 20. Comparison of numerical and experimental relative angular velocity vs time at 35 °C.

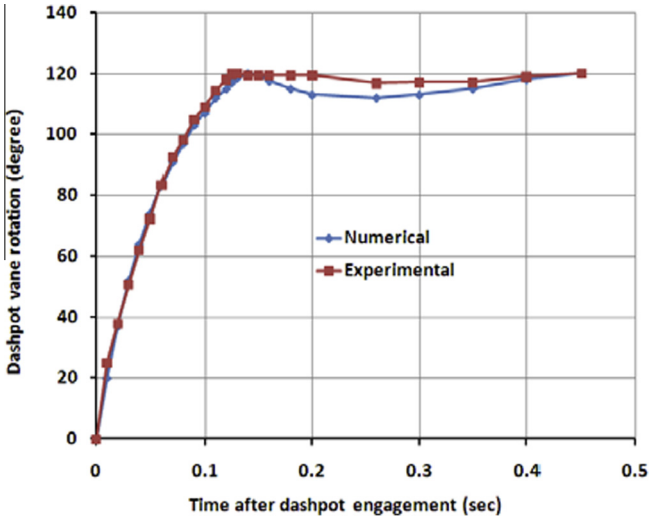

Fig. 21. Comparison of numerical and experimental dashpot vane rotation vs time at 55 °C.

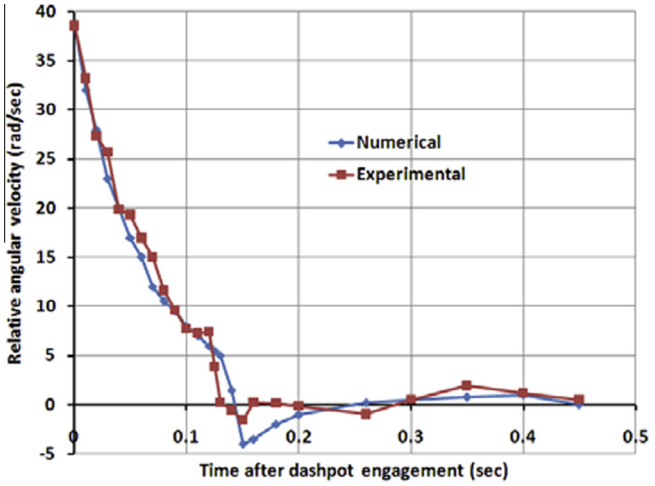

Fig. 22. Comparison of numerical and experimental relative angular velocity vs time at 55 °C.

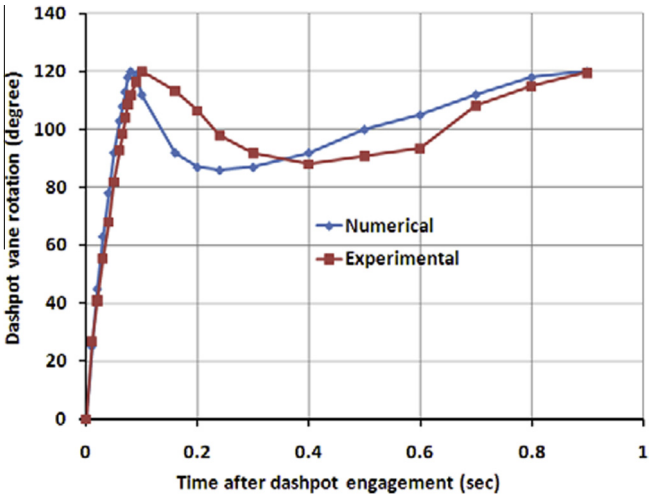

Fig. 23. Comparison of numerical and experimental dashpot vane rotation vs time at 85 °C.

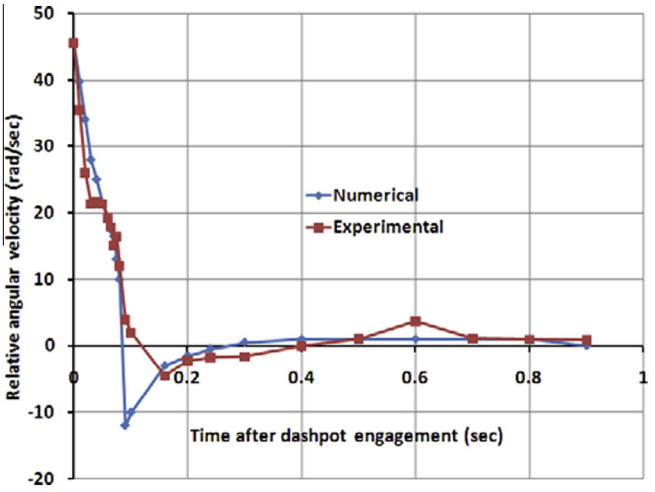

Fig. 24. Comparison of numerical and experimental relative angular velocity vs time at 85 °C.

dashpot rotation and the vane velocity goes smoothly to zero. Relative angular acceleration curve at 35 °C (Fig. 10) shows that the vane decelerates fast initially and then stops smoothly. There is a slight kink when the vane stops with terminal velocity, which is very less at 35 °C. At 55 °C and 85 °C the vane movement sees the impact, as the relative rotation, angular velocity and acceleration curves are not smooth. This shows that the moving vane is hitting the stopper. Relative angular acceleration curves at 55 °C and 85 °C shows erratic acceleration/deceleration behavior as the vane hits the stopper and we see the impact. The impact is more severe at 85 °C. The impact in the dashpot at elevated temperature (55 °C and 85 °C) is due to reduction in the viscosity of oil. At elevated temperature the parameters which are driving the dashpot shaft, like moment of inertia and shut-off rod weight are same as that of 35 °C, but the reduction in the damping moment due to low viscosity results into the impact in the dashpot operation.

Energy variation is analyzed in Figs. 11–13, we can see that, initially the kinetic energy is acquired by the moving vane, which gets converted into the heat and absorbed in the dashpot. So, as kinetic energy reduces with time, energy absorbed by the dashpot increases and saturates. Energy absorbed by the dashpot is more than the kinetic energy, because some heat is also generated due to constant applied moment on the dashpot shaft. Some energy is also absorbed in the spiral spring as shown in energy variation curves (Figs. 11–13). At 55 °C and 85 °C, the energy variation curves also have kink, because of the impact in the dashpot.

As shown in Fig. 7, the temperature rise in dashpot vanes is high at local surfaces which are in relative motion. Because, these surfaces are near the heat source which is energy dissipated in the dashpot operation. The highest temperature rise observed is 5 °C at time = 0.01 s. The temperature rise is locally, while the bulk temperature of dashpot components remains nearly constant. Local temperature rise also reduces gradually with time and found to be negligible at the end of dashpot operation. Because by this time whole energy is absorbed in the dashpot. This temperature analysis is done with the assumption that whole damper heat is transferred in the dashpot components, if some heat goes into the dashpot oil then this temperature rise will be less. The important simulation results are given in Table 2.

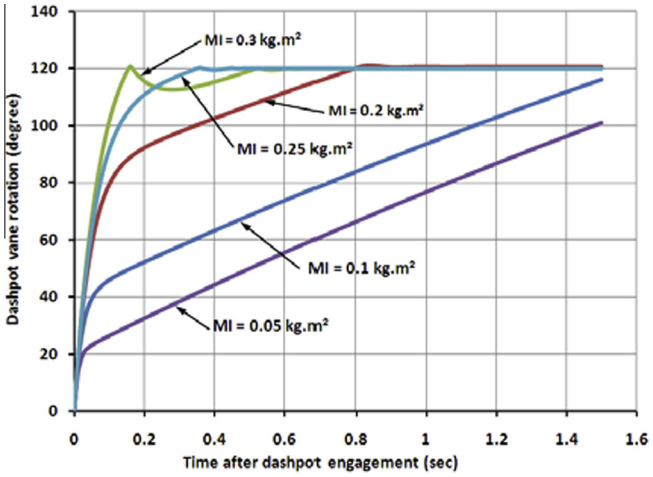

Fig. 25. Variation of dashpot vane rotation vs time with different values of moment of inertia at 35 °C.

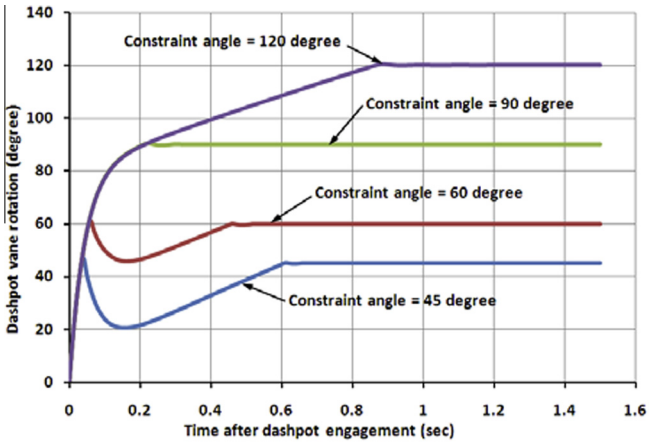

Fig. 26. Variation of dashpot vane rotation vs time with different values of constraint angle at 35 °C.

4. Experimental study

In order to study the dynamics of the hydraulic dashpot experiments were conducted on a full scale test station. Shut-off rod drive mechanism and test station of 'Critical facility' reactor has been used to conduct the experiments. Fig. 14 shows the full scale test-station along with the test console, recorder and heating oven. To record the rod drop profile, rod is taken motorized up, and then EM clutch is deenergized, shut-off rod falls due to gravity, which rotates the sheave, as wire rope is wound on the sheave. Pick-up rings which are mounted on the sheave shaft start picking-up one over the other. These pick-up rings are used to load the dashpot at the end of travel and dashpot attains the initial velocity. Inside view of drive mechanism showing pick-up rings is also given in the Fig. 14. Heating oven was used to conduct the experiments at elevated temperatures. Once the desired temperatures reached the experiments were conducted and dashpot speed, pressure rod positions were measured. Tacho-generators (Make: Servo-tek, Accuracy: 0.571%) is mounted on the mechanism to measure the sheave shaft and dashpot speeds. A potentiometer (Make: Duncan, Linearity: 0.15%) is mounted on the sheave shaft to measure the rod position at any time. A pressure transducer (Make: Schaevitz, Accuracy: 0.059%) is mounted on the hydraulic dashpot to measure the pressure inside the oil chamber. A test console is used to operate the SRDM. PC based recorder (data-logger, Make: DEWEsoft) is used to plot the output voltage of tacho-generators, potentiometer and pressure transducer against time. The output voltages are converted into the sheave shaft angular velocity/hydraulic dashpot angular velocity, rod position and hydraulic dashpot pressure. Experiments were conducted at room temperature as well as at elevated temperatures. Because of limitations of sensors and switches in the drive mechanisms, the experimental study was restricted up to 85 °C. Sensor constants are given below:

Tacho-generator: 1000 RPM/7 V.
Potentiometer voltage variation for full dashpot movement: 3.95 V.
Pressure transducer: 2.5 bar/V.

Experimental results are given in Table 3 and corresponding experimental plots are given in Figs. 15–18 with various conditions. Fig. 15 show the comparison of sheave angular velocity vs time at various temperatures. Similarly, Fig. 16 shows the comparison of dashpot response (angular velocity), Fig. 17 shows the comparison of damping moment due to pressure and Fig. 18 shows the comparison of relative vane rotation at various temperatures.

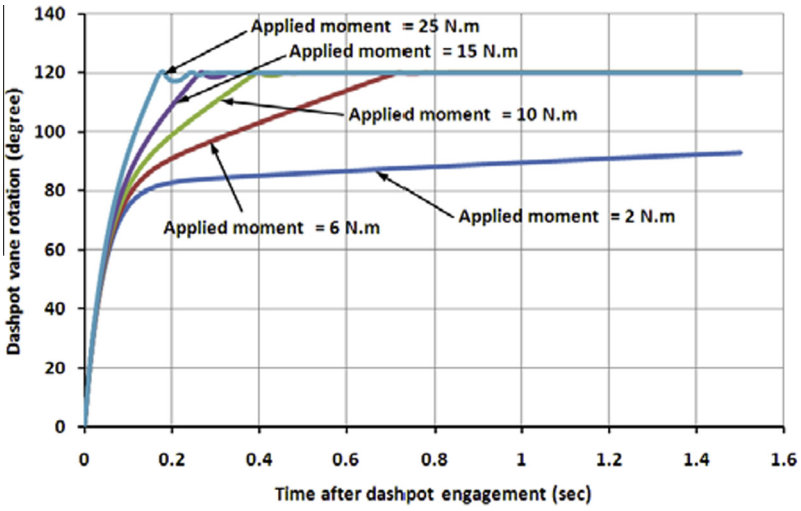

Fig. 27. Variation of dashpot vane rotation vs time with different values of applied moment at 35 °C.

5. Results and discussion

5.1. Discussion on numerical and experimental results

Experimental results at 35 °C, 55 °C and 85° are compared in Figs. 15–18. Impact/kink is clearly visible in the experimental plots at elevated temperatures, which is more severe at 85 °C. Impact is due to reduction in viscosity at elevated temperature. Numerical and experimental results are compared in Figs. 19–24. Results are compared at room temperature (35 °C) as well as at elevated temperatures of 55 °C and 85 °C. Comparison shows that the results are in close proximity at 35 °C all throughout as shown in Figs. 19 and 20. At room temperature, the damping coefficient is more because of high oil viscosity and the dashpot absorbs the energy before reaching the mechanical stopper. Variation in slope of numerical and experimental curves in Fig. 19 is seen, which is due to inaccuracy in model input parameters such as, moment of inertia, spring constant and damping coefficient. While at elevated temperatures of 55 °C and 85 °C, where we see the impact in the dashpot operation due to low viscosity of damping oil. Dashpot vane rotations in Figs. 21 and 23 shows that the vane never crosses the 120° and bounces back from mechanical stopper. Bounce back is more in case of 85 °C, as the vane hitting velocity is more in this case. Numerically there is a constraint at 120° and the movement of the dashpot vane is restricted and vane oscillates. The trend of oscillation is very similar to that of experimental results. This trend can be seen in the Figs. 21–24. Mechanical stopper is modeled as stiff spring, which is approximate, so there is a minor variation in experimental and numerical results as shown in Figs. 21–24.

Both numerical and experimental results shows that the dashpot becomes under damped beyond 55 °C and the impact is seen in the damper responses. This means the modeling of hydraulic dashpot predicts the impact in dashpot accurately. Vane hitting velocity is also predicted by the model as given in Table 2 and the experimental values of vane hitting velocity are given in Table 3. The numerical and experimental values of vane hitting velocity are also in close agreement. The model can be improved further by putting more accurate values of input parameters.

5.2. Parametric studies

The model of the hydraulic dashpot is used to extend the study further numerically to study the effects of various parameters. Fig. 25 shows the variation of dashpot vane rotation vs time with different values of moment of inertia at 35 °C. It clearly shows that if, we increase the moment of inertia of the rotating components while keeping all other parameters same, the dashpot becomes underdamped beyond a value of moment of inertia. Because with more moment of inertia, the energy acquired by the dashpot which needs to be absorbed is more, hence results into the impact in dashpot operation. Fig. 26 shows the variation of dashpot vane rotation vs time with different values of constraint angle at 35 °C. the curve shows that if, we reduce the constraint angle below a value, we get the impact in the hydraulic dashpot, as by that time the whole energy of the dashpot is not absorbed. This is because the dashpot requires some minimum rotation to absorb the acquired energy. Similarly, Fig. 27 shows the variation of dashpot vane rotation vs time with different values of applied moment at 35 °C. The applied moment in the hydraulic dashpot shaft is due to the constant weight of the shut-off rod which is always there in the dashpot action. One can see from the Fig. 27 that, beyond a value of applied moment the dashpot becomes under damped and we see the impact in dashpot operation. Shut-off rod weight gives additional loading on the dashpot, as the moment due to this act against the total dashpot moment given by the dashpot (Eq. (3)).

6. Conclusions

Dynamic model of hydraulic dashpot has resulted into a handy tool to analyze the effects of various parameters on dashpot performance. Impact hitting velocity increases with increase in environmental temperature of hydraulic dashpot as damping coefficient of dashpot reduces. Initial kinetic energy acquired by the hydraulic dashpot is more at higher temperatures as viscosity of oil goes down. Impact at higher temperatures is more severe because of higher initial kinetic energy and less damping coefficient of hydraulic dashpot. With increase in moment of inertia, reduction in constraint angle and increase in constant applied moment an overdamped dashpot system can become underdamped without change in damping and spring coefficients. The instant temperature rise in the dashpot due energy absorption is local and for short duration, while the bulk body temperature remains uniform. The study forms a good tool in designing an optimized hydraulic dashpot for future applications. In the present work, only hydraulic dashpot is modeled as a system with 1 DOF, but in future whole SRDM can be modeled and effects of other SRDM parameters can also be studied.

Acknowledgement

Support from the colleagues in Division of Remote Handling and Robotics, BARC for carrying-out the experiments and valuable inputs & comments from Mr. Karimulla Shaik and Dr. Gaurav Bhutani of BARC are appreciated.

References

[1] N.K. Singh, D.N. Badodkar, M. Singh, Numerical and experimental study of hydraulic dashpot used in the shut-off rod drive mechanism of a nuclear reactor, Nucl. Eng. Des. 273 (2014) 469–482.
[2] B.K. Kumbhar, S.R. Patil, S.M. Sawant, Synthesis and characterization of magneto-rheological (MR) fluids for MR brake application, Eng. Sci. Technol. Int. J. 18 (2015) 432–438.
[3] C.J. Wenzler, Analysis of dashpot performance for rotating control drums of lithium cooled fast reactor concept, NASA technical memorandum, (1972) NASA TM X-67992.
[4] I. Suresh, R. Vijayashree, V. Rajan Babu, S. Raghupathy, P. Chellapandi, Performance analysis of oil dashpot in control and safety rod drive mechanism of prototype fast breeder reactor, in: Proceeding of the 1st International and 16th National Conference on Machines and Mechanisms (iNaCoMM2013), IIT Roorkee, India, Dec 18–20, 2013, pp. 211–216.
[5] R. Bulin, M. Hajzman, P. Polach, Basic model of a control assembly drop in nuclear reactors, Transactions of the VSB-Technical University of Ostrava, Mechanical Series, No. 1 vol. LIX (2013) article No. 1927.
[6] P.J. Allen, A. Hameed, H. Goyder, Automotive damper model for use in multi-body dynamic simulations, Proc. IMechE D J. Automobile Eng. 220 (2006).
[7] A. Lion, S. Loose, A thermomechanically coupled model for automotive shock absorber; theory, experiment and vehicle simulation on test tracks, Veh. Syst. Dyn. 37 (2002) 241–261.
[8] Z. Jingyang, S. Bifeng, W. Jin, Flapping wing multi-body dynamic simulation, Procedia Eng. 99 (2015) 885–890.
[9] A. Shabana, Viscoelastic analysis of multi-body systems using the finite element method, J. Sound Vib. 100 (2) (1985) 271–284.
[10] M. Singh, Design and development of drive mechanisms for adjuster rods, control rods & shut-off rods of TAPP-3&4, Nu-power, Int. J. Nucl. Power 16 (2002) 1–2.
[11] S.S. Taliyan, D.P. Roy, R.B. Grover, M. Singh, G. Govindarajan, Dynamics of rod drop in a PHWR, Nucl. Eng. Des. 147 (1994) 311–319.
[12] COMSOL Multiphysics 5.1 Documentation.
[13] COMSOL tutorial: Stresses and heat generation in landing gear, Model library path: Multibody_Dynamics_Module/Automotive_and_Aerospace/landing_gear.
[14] COMSOL tutorial: Fluid damper, Model library path: CFD_Module/Non-Isothermal_Flow/fluid_damper.
[15] W.T. Thomson, M.D. Dahleh, Theory of Vibrations with Applications, fifth ed., Prentice Hall Publication, 1998, pp. 83–85.
[16] R.B. Bird, W.E. Stewad, E.N. Lightfoot, Transport Phenomenon, second ed., John Wiley & Sons, 2007, pp. 311–317.
[17] M. Asif, A.S. Kulkarni, P. Sathiya, Finite element modeling and characterization of friction welding on UNS S31803 duplex stainless steel joints, Eng. Sci. Technol. Int. J. 18 (2015) 704–712.